Density Functional Theory Study of the Interaction of 2- Mercaptobenzimidazole and Gold, Palladium and Nickel atoms

*Ourida Mahmoudi[1, 2, 3], Tarik Bordjiba[2, 3] * and Abed Mohamed Affoune[3]*

[1]Departement of Chemistry, Sciences Faculty, Badji-Mokhtar-Annaba University, Box 12 , 23000 Annaba, Algeria
[2] Laboratory of Electrical Engineering of Guelma, 8 mai 1945-Guelma University Box 401, 24000 Guelma, Algeria
[3] Process Engineering Department, Sciences and Engineering Faculty, 8 mai 1945-Guelma University, Box 401, 24000 Guelma, Algeria

*E-mail: bordjiba_tarik@yahoo.ca

The purpose of this work is to study the adsorption of 2-Mercaptobenzimidazole on three different types of atoms: gold, palladium and nickel. The Density Functional Theory Study (DFT) calculations were performed on 2-Mercaptobenzimidazole (2MBI) and three complexes: 2-Mercaptobenzimidazole-gold atom (2MBI-Au), 2-Mercaptobenzimidazole-palladium atom (2MBI-Pd) and 2-Mercaptobenzimidazole-nickel atom (2MBI-Ni).The quantum chemical parameters of 2MBI and the complexes: 2MBI-Au, 2MBI-Pd and 2MBI-Ni, have been calculated. The considered quantum chemical parameters are: lengths bonds, angles bonds, optimization energy, binding energy, Mulliken atomic charges, energies of highest occupied molecular orbital (E_{HOMO}), the lowest unoccupied molecular orbital (E_{LUMO}), the energy difference (ΔE) between E_{LUMO} and E_{HOMO}, chemical hardness η and the dipole moment μ. The complexation of 2MBI with Au, Pd and Ni atoms modifies the quantum chemical parameters of the organic molecule. This study reveals that gold atom bonds with 2MBI molecule via sulfur atom, however, the palladium and nickel atoms bond with 2MBI molecule via nitrogen atom. The results of the present work give a new insight on self assembly of 2-Mercaptobenzimidazole molecules at metal surface and provide significant information for fundamental and applied electrochemistry.

1. INTRODUCTION

Recently, self-assembled monolayers (SAMs) have expected an immense interest due to their permanency and easy preparation [1]. The potential application of SAMs consists of several fields such as: sensor fabrication [1, 2-5], ion recognition [1, 6], molecular electronics [1, 7-10], studies of electron transfer kinetics [1, 11, 12], high density memory storage devices [1, 13], biomolecular investigations [1, 14], immobilization of biocatalysts [1,15], electrocatalytic studies [1, 16], mediation of electron transport across molecular films [1, 17, 18], and corrosion protection [1, 19].

Self-assembled monolayers of aliphatic systems have been widely studied in the past years [20], whereas more recently the attention has focused on SAMs of aromatics and hetero-aromatics thiols by molecular electronics applications and by lithography to center on the ultra-short length level [21]. Aromatic thiols SAMs are moreover attractive for the reason of very high electron density and intensive intermolecular interactions [1].

Among the hetero-aromatics thiols, the 2-mercaptobenzimidazole (2MBI) molecule, which is illustrated in Fig. 1, has a simple thiolfunctionnel group that may be expected acting as the main chemisorption center.
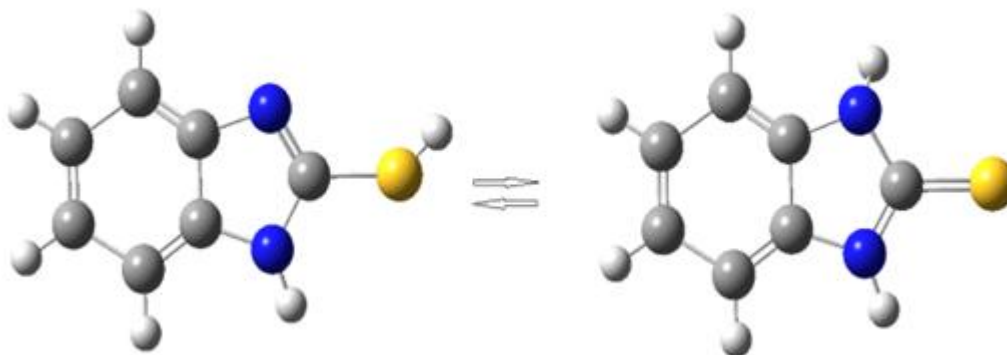

Figure 1. Tautomerization of 2-mercaptobenzimidazole molecule

Additionally, one or mutually of the two nitrogen atoms in the heterocyclic region ring may act as second center for interaction with the surface [22]. The 2MBI molecule could be present in two tautomeric forms [23] (Fig. 1). The sulfur atom is protonated in the thiol form leaving two chemically dissimilar nitrogen heteroatoms one protonated and the other one deprotonated in difference in the thione form where mutually nitrogen atoms are protonated [22].

Most investigations employed gold as a substrate for adsorption of 2-mercaptobenzimidazole molecule because ordered gold films are easy to prepare [24]. Despite many experimental and theoretical investigations on the structure Au-S bond in SAMs prepared of thiolate, the precise nature of the molecule-metal interface is still subject of discussion [25], and there is still insufficient acknowledged concerning the reactions provided SAMs from organosulfur compounds with other metals, for example palladium, nickel, silver, copper, and mercury [26].

Gold is historically the most studied with SAMs and binds thiols with a high affinity [27, 28], but recent studies [24], indicate that functionalized thiols produce anarchic structures on a gold

substrate. These studies reveal the necessity to find other substrates on which thiols of different dimensions could generate stable monolayers with small numbers of imperfections [24]. The look for such substrates has included studies of the adsorption on palladium and nickel, which provide comparable properties, but the SAMs grown on these substrates have been less investigated than those on gold [26].

Palladium looks to be a convenient substitute to gold for various purposes, and it is better than gold for others. While Pd is less considered than the coinage metals (Au, Ag, Cu) as a support for SAMs, it has a sum of important properties, for example, thin layer of palladium consist of grains 2-3 times slighter than those in gold layers. This characteristic is essential for producing nanostructures with low density of imperfections and small border irregularity [26, 29, 30], furthermore it is well suited with complementary metal oxide semiconductor processing; gold is not [31]. The studies of SAMs on palladium as substrate for adherent cells show that the long-term stabilities of these firms are greater than those on gold [26], and finally approximating to Au, Pd does not oxidize at indoor temperature [26, 28].

Nickel (Ni) varies widely from coinage metals, as thiols are incapable to reduce the nickel oxide film to provide thiolate SAMs. It is also motivating to evaluate nickel with other metals from its group (i.e. palladium and platinum). Few investigations of SAM formation on Pt and Pd have been realized in recent times [30-41]. The thiolate SAMs grown on Ni can be compared with the SAMs made on Pd and Pt. Thiolate SAM can be formed on these metals (Ni, Pd and Pt) after passive oxide layer reduction. Nevertheless, coadsorption of a submonolayer of sulfur can moreover happen during SAM formation [30, 32, 33, 37, 40, 42-44]. Several experimental investigations on Ni have shown that an oxide layer of little nanometer thicknesses [32, 45, 46] is impulsively created on contact to atmospheric oxygen. Until this day, just a small number of researches are carried out on organothiols SAMs on Ni support [32, 43, 48-51].

Comprehension of the interaction of 2- Mercaptobenzimidazole and the different types of electrodes such as gold, palladium and nickel open new routes in electrochemistry. In this context, we propose to study the adsorption of 2-mercaptobenzimidazole on three different atom gold, palladium and nickel with the intention to understand and evaluate the interaction between this molecule and the abovementioned metallic atoms. We have used the density functional theory (DFT) [52], methods to determine the quantum chemical parameters such as the Mulliken charges, the highest occupied molecular orbital (E_{HOMO}) and the lowest unoccupied molecular orbital (E_{LUMO}) energies, the difference (ΔE) between E_{LUMO} and E_{HOMO} energy, chemical hardness (η), total energies and dipole moment (μ).

2. COMPUTATIONAL DETAILS

Calculations have been completed by remedying to DFT methods via the Gaussian 09 W set of program. The 2MBI thiol molecule was built by using GaussView program. The geometry of obtained molecular was optimized and the calculations were performed with PBE/LANL2DZ.

In the optimized structure of the 2MBI molecule, the hydrogen atom that bonds by sulfur was substituted by the three different type of metallic atom Au, Pd and Ni in order to simulate the adsorption of the 2MBI molecule on metal atom. The resulting structures were optimized by using the DFT method at the PBE/LANL2DZ level [53-58]. The obtained structures were denoted as 2MBI-Au, 2MBI-Pd and 2MBI-Ni.

Computations of quantum chemical parameters such as: E_{HOMO}, E_{LUMO}, $\Delta E = E_{LUMO} - E_{HOMO}$, chemical hardness η and the dipole moment μ were done at DFT technique level by PBE/LANL2DZ for the organic molecule 2MBI and studied organometallics complexes 2MBI-Au, 2MBI-Pd and 2MBI-Ni for study the adsorption of 2MBI molecule on Gold, Palladium and Nickel atoms.

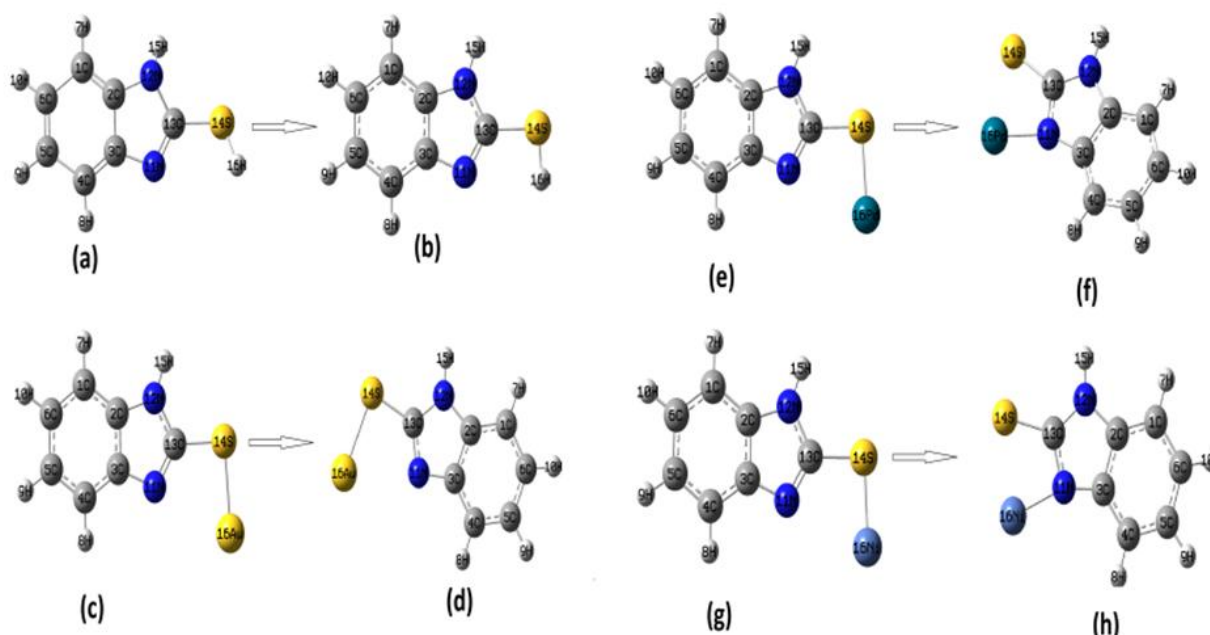## 3. RESULTS AND DISCUSSION

3.1. Molecular geometry

Figure 2. The structure of 2MBI and substituted hydrogen of 2MBI with Au, Pd and Ni (a, c, e and g) respectively. The optimized structures of 2MBI and substituted hydrogen of 2MBI with Au, Pd and Ni (b, d, f and h) respectively.

Fig. 2 shows the structure of 2MBI, 2MBI-Au, 2MBI-Pd and 2MBI-Ni before and after structure optimization. The drawn 2MBI is presented in Fig. 2a and the optimized structure of 2MBI is illustrated in Fig.2b. The main lengths and angles of bonds for the optimized structure of 2MBI are presented in Table 1. In the optimized structure of 2MBI component, S-H, S-C, C-N bond lengths and the HSC, SCN, CNH, SCN(H) bond angles were 1.386A°, 1.816, 1.337, 93.310, 125.658, 126.401, 120.803 respectively using PBE/LANL2DZ which values agree well with experimental and theoretical parameters reported in the literature [59-61] as mentioned in Table1.

The atom of Au as shown in Fig. 2c substituted the hydrogen atom, which binds by sulfur in the optimized structure of 2MBI molecule. This is in order to simulate the adsorption of 2MBI molecule on the gold atom. After the optimization of this structure (Fig. 2d), the Au atom is still bonded to the 2MBI through the sulfur atom. The main lengths and angles of bonds for the optimized structure of 2MBI are shown in Table 2.

Table 1. Comparative selected bond's lengths (A°) and bond's angles (°) for 2MBI experimental and theoretical calculations by DFT. PBE/LANL2DZ.

Bond's lengths	Theoretical Calculations PBE/LANL2DZ	Experimental Reference [59,60]	Theoretical Calculations Reference [61]
H(16)—S(14)	1.386	----------------	1.373
S(14)—C(13)	1.816	1.684, 1.6715	1.812
C(13)—N(11)	1.337	1.362, 1.365	1.393
C(13)—NH(12)	1.399	1.383	-------
NH(12)—H(15)	1.018	1.050	1.010
NH(15)—C(2)	1.408	1.383, 1.389	
N(11)—C(3)	1.419	---------------	
C(2)—C(3)	1.437	1.384, 1.400	
H(16)—N(11)	2.692	----------------	
Bond's angles	Theoretical Calculations PBE/LANL2DZ	Experimental Reference (69,70)	Theoretical Calculations Reference (71)
H(16)—S(14)—C(13)	93.310	---------------------	94.200
S(14)—C(13)—N(11)	125.658	126.800, 127.200	
C(13)—N(11)—C(3)	106.828	111.000 ,110.400	
C(13)—N(12)—H(15)	126.401	121.000	126.200
C(13)—NH(12)—C(2)	104.557	110.400, 110.000	
S(14)—C(13)—NH(12)	120.803	126.800, 127.200	120.700
N(11)—C(13))—N(12)	113.544	---------------------	113.300

Table 2. Comparative selected bond's lengths (A°) and bond's angles (°) for 2MBI, 2MBI-**Au**, 2MBI-**Pd** and 2MBI-**Ni** by DFT.PBE/LANL2DZ.

Bond's lengths\Complex	2MBI	2MBI-**Au**	2MBI-**Pd**	2MBI-**Ni**
M(16)—S(14)	1.386[H-S] bonded	2.403[Au-S] bonded	2.609[Pd-S] unbounded	2.415[Ni-S] unbounded
S(14)—C(13)	1.816	1.810	1.781	1.782
C(13)—N(11)	1.337	1.349	1.364	1.371
C(13)—NH(12)	1.399	1.397	1.389	1.387
NH(12)—H(15)	1.018	1.018	1.018	1.018
NH(12)—C(2)	1.408	1.409	1.413	1.431
N(11)—C(3)	1.419	1.416	1.407	1.407
C(3)—C(2)	1.437	1.438	1.439	1.439
M(16)—N(11) M:H,Au, Pd,Ni	2.692[H-N] unbonded	2.929[Au-N] unbonded	2.093[Pd-N] bonded	1.944[Ni-N] bonded
Bond's angles\Complex	2MBI	2MBI-**Au**	2MBI-**Pd**	2MBI-**Ni**
M(16)—S(14)—C(13)	93.310	94.195	100.163	95.332
S(14)—C(13)—N(12)	125.658	125.901	117.804	117.978
C(13)—N(12)—C(2)	106.828	105.040	107.972	107.629
C(13)—N(12)—H(15)	126.401	126.281	124.812	124.685
C(13)—N(11)—C(3)	104.557	106.807	108.234	108.410
S(14)—C(13)—NH(12)	120.803	120.759	132.101	131.947
N(11)—C(13))—N(12)	113.544	112.330	110.099	110.075

We note that the optimized S-Au, S-C, C-N bond lengths and the optimized AuSC, SCN, CNH, SCN(H) bond angles in the complex 2MBI-Au were 2.403A°, 1.810A°, 1.349A°, 94.195°, 125.901°, 126.281°, 120.759°, respectively. A little variation is observed on the important bond lengths and angles comparatively with component 2MBI.

With the intention of simulation the adsorption of 2MBI on palladium, the hydrogen atom which binds by sulfur in 2MBI was substituted by the atom of Pd (Fig. 2e); the result of optimization is presented in Fig. 2f. We observe that palladium atom is broken from sulfur and bonded with deprotonated nitrogen. The mainly lengths and angles of bonds for the optimized structure of 2MBI-Pd complex are shown in Table 2. We note that the optimized N-Pd, S-C, C-N bonds lengths and the optimized PdNC, SCN, CNH, SCN(H) bonds angles in the complex 2MBI-Pd were 2.093A°, 1.781A°, 1.364A°, 100.163°, 117.804°, 124.812°, 132.101°, respectively. We note the variation on the significant bonds lengths and angles comparatively with component 2MBI and the complex 2MBI-Au.

Fig. 2g presents the replacement of the hydrogen atom by nickel atom in 2MBI; the optimized structure of 2MBI-Ni is shown in Fig. 2h. We note that the nickel atom is also broken from sulfur and bonded with deprotonated nitrogen. We note nearly the same bond lengths and angles comparatively au complex 2MBI-Pd.

3.2. Optimization energy and Binding energy

From the optimized structures of 2MBI, 2MBI-Au, 2MBI-Pd, 2MBI-Ni, several parameters can be explored. Optimization energy, binding energy and lengths between sulfur or nitrogen and metal ('S' or 'N' and M) are presented in Table 3.

Table 3. Optimisation energy of complexes and metal atom, adsorption energy, binding energy and length between sulfur 'S' or nitrogen 'N' and metal ' M'.by DFT. PBE/LANL2DZ.

Complex 2MBI—M	Optimisation energy of Complex 2MBI- M (a.u.)	Optimisation energy of metal atom (Au, Pd and Ni) (a.u.)	Adsorption Energy (a.u.)	Binding Energy (a.u.)	Distance S—M(H) (A°)	Distance N—M(H) (A°)
2MBI S—H	-389.44409				1.386 bonded	2.692 Unbonded
2MBI-Au S—Au	-524.77041	-135.41879	-0.09247	0.09247	2.403 bonded	2.929 Unbonded
2MBI-Pd N—Pd	-515.60731	-126.67396	-0.51074	0.51074	2.609 unbonded	2.093 Bonded
2MBI-Ni N—Ni	-558.19288	-168.94533	-0.19654	0.19654	2.415 unbonded	1.944 Bonded

The binding energy of the 2MBI thiol molecule to the metal atom was determinate by using the following eq [62]:

$$E_{binding} = -E_{adsorption} \qquad (1)$$

Where $E_{adsorption} = E_{2MBI-M} - (E_{atom} + E_{2MBI})$

And E_{2MBI-M} is the total energy of the complex (metal atom and the molecule 2MBI); E_{atom} is the energy of the metal atom and E_{2MBI} is the energy of the molecule 2MBI.

The results given in Fig. 2c-d show that gold atom is still bonded to the 2MBI by sulfur even after optimization. The bond length between S and Au atoms is equal to 2.403A°, the total energy optimization is evaluated to -524.77041a.u. and binding energy is equal to 0.09247a.u. After the

structure optimization of 2MBI-Pd, the palladium atom is ruptured from the S atom and bonds to nitrogen atom.The bond length between N and Pd equal to 2.093A° with total energy optimization equivalent to -515.60730a.u. and binding energy equal to 0.51074a.u. In the optimized structure of the 2MBI-Ni, the nickel atom is broken from the S atom and bonded to the nitrogen atom and the length bond between N and Ni is equal to 1.944A° with total energy optimization equal to -558.19288a.u. and binding energy equal to 0.19654a.u.

The order for the binding energy is the following: E_{bindig}(2MBI-Au)<E_{bindig} (2MBI-Ni) <E_{bindig} (2MBI-Pd).These reveals that Pd-N bond is stronger than Ni-N bond which is stronger than Au-S bond.

The bonding of gold to sulfur and palladium, nickel to the nitrogen atom of 2MBI can be explained by the electronic configuration of gold, palladium and nickel atoms. The electronic configuration of gold atom Au(0) is described as $[Xe]4f^{14}5d^{10}6s^1$ [63] the last orbital $6s^1$ is occupied by one electron, so this atom can donate and accept one electron to become more stable as shown in the following configuration$[Xe]4f^{14}5d^{10}s^2$. Furthermore, the donate electron is given to sulfur atom of the molecule 2MBI this is why after optimization of the structure of the complex 2MBI-Au, gold is still bonded with sulfur of the molecule 2MBI. The frees electrons of gold atom Au(0) and the sulfur atom S of the molecule 2MBI can be the origin of the covalent bond. From the work of [64], while —SH is adsorbed on the gold surface; the hydrogen atom is removed and the powerful Au—S covalent bond is subsequently constitute.

The electronic configuration of the palladium Pd(0) is represented by $[Kr]4d^{10}5s^0$ [65]. We observe that the latest orbital $5s^0$ is free of electrons and it can accept two electrons, which can be provided by the free electronic doublet of deprotonated nitrogen atom of 2MBI molecule. This is in order to allow to Pd atom to have the stable configuration as $[Kr]4d^{10}5s^2$. This is why after the optimization of the structure of the complex 2MBI-Pd, palladium atom is broken from sulfur and bonded with nitrogen atom of the molecule 2MBI.

The electronic configuration of the Ni is represented by $[Ar]3d^84s^2$. We observe that the latest orbital $3d^8$ has the fifth case vacant. This orbital can accept two electrons that can be given from the free electronic doublet of deprotonated nitrogen atom of the molecule 2MBI to allow to the atom of nickel to have more stable configuration as $[Kr]3d^{10}4s^2$. This is why after optimization of the structure of 2MBI-Ni, nickel atom is ruptured from sulfur and bonded with nitrogen atom of 2MBI.

We note that electronic configuration of both palladium and nickel has the same structure $[Kr](4d, 5s)^{10}$ and $[Ar](3d, 4s)^{10}$ respectively and the identical number of valence electron.

In this study, there are two different donor atoms, sulfur and nitrogen. According to[66-68], when bi-functional ligands with two donors atoms are utilized, the gold atom will bind to these ligands through the atom with the higher donor strength according to the order Si~P> C > S >Cl> N > O > F. In other words, the two bi-functional are coordinated to Au through the P and S atoms but not N, since P and S are better soft donor than N [69].

Table 4. Calculated Mulliken atomic charges of 2MBI and 2MBI-Au, 2MBI-Pd, 2MBI-Ni by DFT. PBE/LANL2DZ.

2MBI	2MBI-Au	2MBI-Pd	2MBI-Ni
16 H 0.151	16 Au 0.068	16Pd 0.205	16 Ni 0.242
14 S -0.004	14 S 0.038	14 S 0.003	14 S -0.018
13 C -0.178	13 C -0.058	13 C -0.096	13 C -0.099
12 N -0.405	12 N -0.411	12 N -0.388	12 N -0.376
11 N -0.028	11 N -0.059	11 N -0.267	11 N -0.288

Additionally, the gold is frequently defined as a soft metal and consequently, might be estimated to prefer soft donor ligands for example S and C to the hard donor ligands such as those bonding through N or O [70]. Consequently, it was usually supposed that Au (I) would not efficiently coordinate to a donor N atom [66-68].

The Pd and Ni atom favor binding with N which more electronegative than S. The electronegativity of N and S are 3.0 and 2.5 respectively [65].

From the Table 4, the charge of nitrogen in the molecule 2MBI is much higher than that of sulfur (the charges for N and S are -0.028 and -0.004 respectively). This confirms that nitrogen is more electronegative than sulfur. Presumably, the nitrogen constitutes a Lewis base rich in electrons and forms a donor by mesomeric effect.

3.3. Mulliken atomic charges

Only the main charges were considered, so the charges above the two nitrogen atoms, sulfur, carbon linked to the sulfur and metallic atoms are given in Table 4.

The PBE/LANL2DZ method is used to estimate the Mulliken atomic charges for the organic molecule and the complexes. For the optimized molecule 2MBI, the sulfur atom carries a weak negative charge -0.004 and the two nitrogen atoms carry the negative charges whose values are -0.028 for deprotonated nitrogen and -0.405 for nitrogen bonded with hydrogen. These results show that sulfur and nitrogen atoms are sites, which can give electrons to the substrate atom to donate a coordination type further reaction with these atoms that have free of bond, and these can undergo doublet electrons. It was demonstrated that local electron densities are indispensable in several chemical responses and physicochemical characteristics of compounds [71]. Adsorption of organic molecules can be explicated by the interaction of these molecules with metal atom.

For the calculated Mulliken atomic charges of complex 2MBI-Au, the charges distribution has changed comparatively to that one of the molecule 2MBI. Therefore, we distinguished an increase of atomic charge of the exocyclic sulfur, which becomes 0.038 instead of -0.004 after being linked to gold atom whose charge is positive and equal to 0.068. It have been cited that in the formation process of SAM from thiols (i.e., R-SH), the hydrogen atom is take away during SAM development, and a covalent sulfur-gold bond is created displaying extremely small charge transfer between metal and sulfur [72].The nitrogen atoms charges decreased strongly for deprotonated nitrogen whose value

charge change into -0.059 and weakly for nitrogen bonded with hydrogen whose charge value becomes -0.411 and this will be explained by attracter inductive effect for sulfur to equilibrium the charge of gold. The molecule 2MBI is adsorbed to gold atom via sulfur through the thiol tautomer.

The charge distribution of the complex 2MBI-Pd is different of that one of the organic molecule 2MBI. In this complex, the atomic charge of sulfur is 0.003 instead of -0.004 in the 2MBI molecule. Also, the atomics charges of the two nitrogen atoms are modified to be -0.267 and -0.388 respectively. After the adsorption the organic molecule 2MBI on the Pd atom, the negative charge of deprotonated nitrogen atom increased strongly and this can be explicated by the attracter inductive effect of the nitrogen through its conjugate doubled bond with carbon, while the charge of protonated nitrogen decreased. This increase of charges deprotonated nitrogen has the aim to balance the charge of palladium atom, which is 0.205. 2MBI molecule is adsorbed on the palladium atom via deprotonated nitrogen.

For the calculated Mulliken atomic charges values of the 2MBI-Ni complex, we note the same observation as that one of the 2MBI-Pd complex except for the sulfur atom charge, which is negative and equal to -0.018. In addition, the atomic charge of the Ni atom is estimated to 0.242 after its bonding with deprotonated nitrogen that has a charge of -0.288. However, the atomic charge of the protonated nitrogen is –0.376. Therefore, the thiol form of the molecule 2MBI is likely to react chemically with nickel atom through deprotonated nitrogen atom.

The comparison of charge distribution of the three complexes show that the atomic charges of the two reactive sites sulfur and deprotonated nitrogen follows this order: atomic charge of the sulfur for the 2MBI-Au is higher than the sulfur atom in the complexes 2MBI-Pd and 2MBI-Ni. This is due to the aim to equilibrate charge between sulfur and gold in the complex 2MBI-Au.

While the atomic charges of deprotonated nitrogen is higher for the complex 2MBI-Pd and 2MBI-Ni than that of the complex 2MBI-Au. It seems that this behavior is to equilibrate charges between deprotonated nitrogen and palladium or nickel in the complex 2MBI-Pd and 2MBI-Ni.

Additionally, we observe that the charge distribution of the complexes 2MBI-Pd and 2MBI-Ni is nearly similar. The atoms Pd and Ni are linked with the same atom deprotonated nitrogen of 2MBI while the charge distribution of 2MBI-Au is different because the gold atom is bonded with sulfur atom. Moreover, we distinguish that adsorption of organic molecule on metal atom change the charge distribution of the organic molecule 2MBI.

3.4. HOMO, LUMO, Gap energy and dipole moment

The calculated quantum chemical parameters E_{HOMO}, E_{LUMO}, gap energy, total energy, dipole moment and chemical hardness for the organic molecule 2MBI, 2MBI with hydrogen atom removed denoted 2MBI⁻, the complexes 2MBI-Au, 2MBI-Pd and 2MBI-Ni are presented in Table 5.

Table 5. Calculated total energy, orbital energies E_{HOMO} and E_{LUMO}, gap energy ΔE, Chemical hardness η and dipole moment μfor 2MBI, 2MBI·, 2MBI-**Au**, 2MBI-**Pd**, and 2MBI-**Ni**. by DFT. PBE/LANL2DZ

2MBI and 2MBI-M (M is Au, Pd or Ni)		E_{HOMO} (eV)	E_{LUMO} (eV)	Gap energy ΔE (eV)	Chemical hardness η (eV)	Dipole moment μ (Debeyes)	Total energy (a.u.)	Total energy (eV)
2MBI		-5.38029	-1.43705	3.94356	1.97178	2.3748	-389.44409	-10597.55271
2MBI·		-5.62581	-1.99926	3.62654	1.81327	5.5144	-388.83676	-10581.02601
2MBI-Au		-5.88514	-3.77675	2.10839	1.05419	0.4888	-524.77041	-14280.00523
2MBI-Pd	α	-4.73160	-2.56881	2.16281	1.08140	2.2314	-515.60731	-14030.70583
	β	-4.57733	-3.86791	0.70942	0.35471			
2MBI-Ni	α	-4.20942	-2.49398	1.71544	0.85772	2.1913	-558.19288	-15189.54462
	β	-3.64586	-2.90086	0.74500	0.37250			

The results obtained by PBE/LANLD2Z method show that the 2MBI· displays the higher value of HOMO energy (E_{HOMO}= -5.62581 eV) than that one of the molecule (E_{HOMO}= -5.38029 eV). Additionally, the gap energy of the 2MBI· (3.62654 eV) is lower than that of the molecule (3.94356 eV). These indicating the capacity of the 2MBI· to donate electrons to the convenient metal atom more than the molecule 2MBI.

The high E_{HOMO} values show that the molecule has a trend to offer electrons to convenient acceptor with low energy vacant molecular orbital. Increasing values of the E_{HOMO} make easy adsorption by influencing the transport process through the adsorbed film; low E_{LUMO} energy indicates the capacity of the molecules to accept electrons [72, 73].

Low values of the energy band gap ΔE [73, 74] allows better adsorption and facilitate bond with metal atoms, for the reason that the energy to extract an electron from the last occupied orbital will be low [75]. Cherry et *al.*[76] have used the notion of LUMO-HOMO energy gap in developing theoretical models [75] which is able to explicate the structure and conformation barriers in various molecular systems [77] qualitatively. According to the results of this study, the 2MBI· is more reactive than 2MBI, this is why we have chosen substitute directly hydrogen atom of 2MBI by one atom of the following element: gold, palladium and nickel. Additionally, the dipole moment μ of the 2MBI· is higher than that one of the organic molecule 2MBI (table 5). This confirms that 2MBI is adsorbed under 2MBI with hydrogen atom removed form and covalent bond is then formed [64].

Furthermore, increasing values of E_{HOMO} and μ make possible adsorption by facilitate the transport process through the adsorbent layer [78]. Nevertheless, the elevate component polarity (dipole moment equal to 2.3748 and 5.5144 for 2MBI and 2MBI·, respectively) makes easy electrostatic interaction between the electric field due to the metal charge and the electric moment of these compounds, and participates to their better adsorption [79, 80].

From table 5, we can seen that the replacement of hydrogen atom in 2MBI by gold, palladium and nickel, change the levels of energies (HOMO, LUMO, gap energy).

The complex 2MBI-Au shows the lowest value of E_{HOMO} comparatively to the HOMO of the two other complexes. This is can be an indication that the complex 2MBI-Au is less donor than the two other complexes under investigation. The LUMO energy of the orbital β of the complex 2MBI-Pd is the lowest of that one of the studied complex. Presumably, the complex 2MBI-Pd may be a good

acceptor. The gap energy of the orbital β of the complex 2MBI-Pd is the lowest than the gap energy of the complexes 2MBI-Au and 2MBI-Ni. This means that the complex 2MBI-Pd can be more reactive with the appropriate donor than the two other complexes.

The energy gap ΔE of the complexes formed 2MBI-Au, 2MBI-Pd(α), 2MBI-Ni(α), 2MBI-Pd(β) and 2MBI-Ni(β) comparatively with the 2MBI molecule obeys the following order:

ΔE(2MBI)>ΔE(2MBI-Pd(α))>ΔE(2MBI-Au)>ΔE(2MBI-Ni(α))>ΔE(2MBI-Ni(β))>ΔE(2MBI-Pd(β)) ie the gap energy for all the complexes is smaller than the gap energy of 2MBI. This offers those complexes to react with the second functionality.

Another parameter of reactivity indication, the chemical hardness η, could be determined according to the subsequent equation [81]:

$$\eta = \Delta E/2 \qquad\qquad (2)$$

The chemical hardness gives the information about the reactive behavior of the complex. Therefore, the reactivity follows this order:

2MBI-Pd(β)>2MBI-Ni(β)>2MBI-Ni(α)>2MBI-Au >2MBI-Pd(α).

From the table 5, the dipole moment μ of the three complexes is low than that one of the organic molecule 2MBI. This reveals that after its adsorption the dipole moment of the molecule decreases.

The forms HOMO and LUMO of the organic molecule 2MBI and complexes under investigations are showing in Fig. 3.
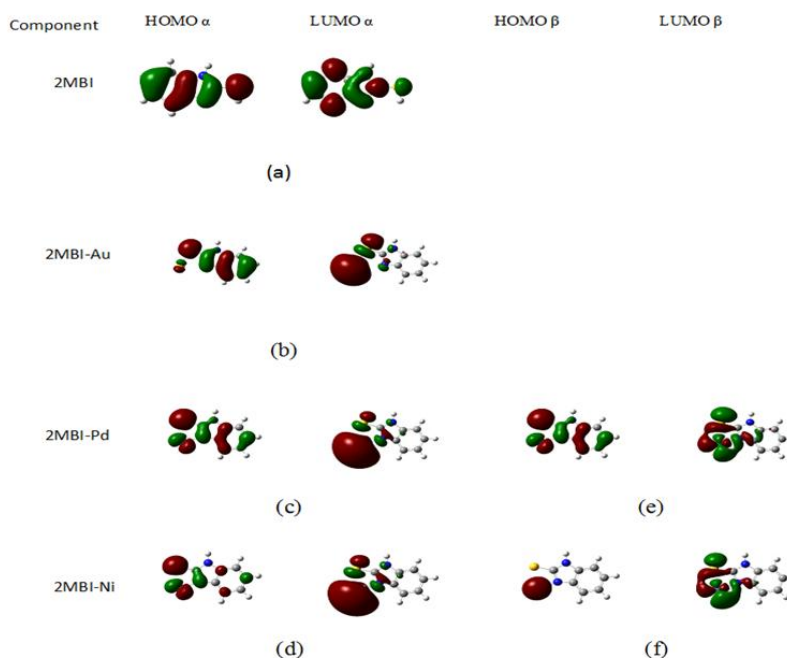

Figure 3. Frontier molecular orbital diagrams of 2MBI and 2MBI-Au, 2MBI-Pd and 2MBI-Ni. a-Orbital diagrams HOMO(α) and LUMO(α) of optimized 2MBI, b-Orbital diagrams HOMO(α) and LUMO(α) of optimized 2MBI-Au, c-Orbital diagrams HOMO(α) and LUMO(α) of optimized 2MBI-Pd, d-Orbital diagrams HOMO(α) and LUMO(α) of optimized 2MBI-Ni. e-Orbital diagrams HOMO(β) and LUMO(β) of optimized 2MBI-Pd, f-Orbital diagrams HOMO(β) and LUMO(β) of optimized 2MBI-Ni.

According to [82] it is recognized that the reactivity of a molecule depends on molecular orbital distribution. HOMO is habitually related with the electron donate aptitude of a molecule, while LUMO shows its aptitude to win electrons [82]. It can be seen from Fig.3(a) that the densities of both HOMO and LUMO of 2MBI molecule are comparatively the same on the entire area of the molecule due to the distribution of π-electron cloud on the molecule. The HOMO density is elevated in the region close to the imidazole ring and thiol group, which is qualified to the existence of electron pairs in the N atoms of imidazole ring [82] and sulfur atom. Therefore, the preferable active centers for giving electrons in 2MBI are principally situated inside the regions approximately nitrogen and sulfur atoms. The LUMO densities on the C–C area in 2MBI molecule are elevated, demonstrating that the favored active centers for wining electrons are principally situated inside this area [82].

For the 2MBI-Au complex Fig. 3(b), the HOMO density is delocalized and essentially distributed on the imidazole section and on the sulfur atom while the population of LUMO is localized on the gold atom and it is obviously superior than that on the imidazole section and sulfur. It is rational to deduce that the sulfur in 2MBI molecule acts as the principal site to offer electrons and generate the coordinated bond with unoccupied d-orbital's of the gold atom.

For the 2MBI-Pd(α) complex Fig.3(c), the HOMOα density is delocalized and is principally distributed on the imidazole section nearby deprotonated nitrogen and on the sulfur atom while the population of LUMOα is principally localized on the palladium atom and it is distinctly elevated than that on the imidazole section and sulfur. It is plausible to presume that the deprotonated nitrogen in 2MBI molecule acts as the principal center to offer electrons and forms the coordinated bond with unoccupied d-orbitals of the palladium atom, which the more appropriate to gain electron.

For the 2MBI-Ni(α)complex Fig. 3(d), the HOMOα density is principally distributed on the nitrogen deprotonated and on the sulfur atom in 2MBI while the population of LUMOα is localized on the nickel atom and it is clearly elevated than that on the nitrogen deprotonated and sulfur. Consequently, it is possible to suppose that the deprotonated nitrogen in 2MBI molecule acts as the main center to offer electrons and generate the coordinated link with unoccupied d-orbitals of the nickel atom which the more appropriate to get electron.

For the 2MBI-Pd(β) complex Fig. 3(e), the shape of HOMOβ density is the same like the HOMOα density Fig. 3(a) while the population of LUMOβ is localized on the sulfur atom and it is elevated and symmetric on the palladium atom and deprotonated nitrogen atom.

For the 2MBI-Ni(β) complex Fig. 3(f), the HOMOβ density is localized only on the nickel atom while the shape of LUMOβ density is the same like the LUMOβ density of the 2MBI-Pd(β) complex.

From these figures, it can be concluded that the compound 2MBI is adsorbed on the gold, palladium and nickel surface via nitrogen or sulfur by using the benzimidazole-thiol moiety, which contains the heteroatoms and aromatic rings. Moreover, the presence of metal atoms affects significantly the molecular orbitals.

The results of the present investigation give several new insights in fundamental and applied electrochemistry such as: (i) Comprehension of the adsorption of 2- Mercaptobenzimidazole on electrodes and investigation of the properties of the monolayers formed at the electrochemical metal-solution interface. This study shows that gold atom bonds with 2- Mercaptobenzimidazole molecule

via sulfur atom, however, the palladium and nickel atoms bond with 2- Mercaptobenzimidazole molecule via nitrogen atom; this finding can contribute to explanation of several electrochemical reactions. (ii) Study of electron transfer for charged thiols molecules. The quantum chemical parameters of 2MBI and the complexes: 2MBI-Au, 2MBI-Pd and 2MBI-Ni contribute to the study of electron transfer trough electrode electrolyte interface. (iii) Application in electrocatalysis by protection of metal catalyzer with thiols molecules layer. The results of this work show that the presence of metal atoms affects significantly the molecular orbitals and by consequences the reactivity of the modified metal electrode. (iv) Study of electrochemical interfaces phenomena of electrodes based on gold, palladium and nickel.

4. CONCLUSIONS

To summarize, the study of the intercation of 2-Mercaptobenzimidazole and gold, palladium and nickel atoms has performed by means of Density Functional Theory. The quantum chemical parameters of 2MBI and the complex 2MBI-Au, 2MBI-Pd and 2MBI-Ni, have calculated. The considered quantum chemical parameters are: length's bonds, angles bonds, optimization energy, binding energy, Mulliken atomic charges, E_{HOMO}, E_{LUMO}, $\Delta E = E_{LUMO}-E_{HOMO}$, chemical hardness η and dipole moment μ. The complexation of 2MBI with Au, Pd and Ni atoms modifies the quantum chemical parameters. This study reveals that gold bonds with 2MBI molecule via sulfur atom, however, the palladium and nickel atoms bond with 2MBI molecule via nitrogen atom. In the future work, we will study the adsorption of 2-Mercaptobenzimidazole on the cluster and thin films of several metals.

References

1. R. K. Shervedani, F. Yaghoobi, A. Hatefi-Mehrjardi, S. M. Siadat-Barzoki, *Electrochim. Acta,* 53 (2008) 4185.
2. S. Sengupta, D. Patra, I. Ortiz-Rivera, A. Agrawal, S. Shklyaev, K. K. Dey, U. Córdova-Figueroa, T. E. Mallouk and A. Sen, *Nat. Chem.*, 6 (2014) 415.
3. L. Liu, Y. Xing, H. Zhang, R. L. Liu, H. J. Liu, N. Xia, *International Journal of Nanomedicine,* 9 (2014) 2619.
4. L. Basabe-Desmonts, J. Beld , R. S. Zimmerman , J. Hernando, P. Mela, M. F. G. Parajo, N. F. van Hulst , A. van den Berg , D. N. Reinhoudt and M. Crego-Calama, *J. Am. Chem. Soc.,* 126 (2004) 7293.
5. H.-C. Wang, H. Zhou, B. Chen, P. M. Mendes, J. S. Fossey, T. D. James and Y.-T. Long, Analyst, 138 (2013) 7146.
6. R. K. Shervedani, A. Farahbakhsh, M. Bagherzadeh, *Anal. Chim. Acta,* 587 (2007) 254.
7. L. Newton, T. Slater, N. Clark and A. Vijayaraghavan, *J. Mater. Chem. C,* 7(2013) 76.
8. M. F. Galhoun, J. Sanchez, D. Olaya, M. E. Gershenson and V. Podzorov, *Nat. Mater.*, 7 (2008) 84.
9. L. Sun, Y. A. Diaz-Fernandez, T. A. Gschneidtner, F. Westerlund, S. Lara-Avilab and K. Moth-Poulsen, *Chem. Soc. Rev.,* 43 (2014) 7378.
10. G. Jia, A. Sitt, G. B. Hitin, I. Hadar, Y. Bekenstein, Y. Amit, I. Popov and U. Banin, *Nat. Mater.,* 13 (2014) 301.

11. J. N. Richardson, S. R. Peck Larry, S. Curtin, L. M. Tender, R. H. Terrill, M. T. Carter and R. W. Murray, G. K. Rowel and S. E. Creager, *J. Phys. Chem.*, 99 (1995) 766.
12. L.V. Protsailo, W.R. Fawcett, *Electrochim. Acta,* 45 (2000) 3497.
13. J. H. Fendler, *Chem. Mater.*, 13 (2001) 3196.
14. J. B. Wood, M. W. Szyndler, A. R. Halpern, K. Cho, and R. M. Corn, *Langmuir,* 29 (2013) 10868.
15. P. N. Ciesielski, A. M. Scott, C. J. Faulkner, B. J. Berron, D. E. Cliffel, and G. K. Jennings, *A.C.S. Nano*, 02 (2008) 2465.
16. X. Xiao, S. Pan, J. S. Jang, F.-R. F. Fan, and A. J. Bard, *J. Phys. Chem. C*, 113 (2009) 14978.
17. V. Ganesh, M. P. C. Sanz, J. C. Mareque-Rivas, *Chem. Commun.*, 8 (2007) 804.
18. R. K. Shervedani, S. A. Mozaffari, *Anal. Chem.,* 78 (2006) 4957.
19. S. Devillers, A. Hennart, J. Delhalle, and Z. Mekhalif, *Langmuir,* 27 (2011) 14849.
20. Y.-T. Long, H.-T. Rong, M. Buck, M. Grunze, *Electroanal. Chem.*, 524-525 (2002) 62.
21. S. Laricchia, F. Ciriaco, L. Cassidei, and F. Mavelli, *Sensor Lett.*, 8 (2010) 521.
22. C. M. Whelan, M. R. Smith, C. J. Barnes, N. M. D. Brown, C. A. Anderson, *Appl. Surf. Sci.*, 134 (1998) 144.
23. M. Gholami, I. Danaee, M. H. Maddahy and M. RashvandAvei, *Ind. Eng. Chem. Res.*, 52 (2013) 14875.
24. N. Mohtat, M. Byloos, M. Soucy, S. Morin, M. Morin., *Electroanal. Chem.,* 484 (2000) 120.
25. J. Kučera and A. Gross, *Langmuir,* 24 (2008) 13985.
26. X. Jiang, D. A. Bruzewicz, M. M.Thant, G. M. Whitesides, *Anal. Chem.*, 76 (2004) 6116.
27. R. G. Nuzzo and D. L. Allara, *J. Am. Chem. Soc.*, 105 (1983) 448.
28. J. C. Love, L. A. Estroff, J. K. Krebel, R. G. Nuzzo, G. M. Whitesides, *Chem. Rev.*, 105 (2005) 1103.
29. A. Carvalho, M. Geissler, H. Schmid, B. Michel and E. Delamarche, *Langmuir,* 18 (2002) 2406.
30. J. C. Love, D. B. Wolfe, M. L. Chabinyc, K. E. Paul and G. M. Whitesides, *J. Am. Chem. Soc.*, 124 (2002) 1576.
31. S. Wolf, Silicon processing for the VLSI Era, Lattice Press, Sunset Beach (1990).
32. S. Rajalingam, S. Devillers, J. Dehalle and Z. Mekhalif, *Thin Solid Films*, 522 (2012) 247.
33. D.Y. Petrovykh, H. K. Suda, A. Opdahl, L. J. Richter, M. J. Tarlov, L. J. Whitman, *Langmuir*, 22 (2006) 2578.
34. M. Geissler, J. Chen, Y. Xia, *Langmuir,* 20 (2004) 6993.
35. J. A. Williams, C. B. Gorman, *J. Phys. Chem. C*, 111 (2007) 12804.
36. T. R. Soreta, J. Strutwolf, C. K. O'Sullivan, *Langmuir*, 23 (2007) 10823.
37. P. Carro, G. Corthey, A. A. Rubert, G. A. Benitez, M. H. Fonticelli, R. C. Salvarezza, *Langmuir,* 26 (2010) 14655.
38. T. Laiho, J. Lukkari, M. Meretoja, K. Laajaleho, J. Kankare, *J. A. Leiro, Surf. Sci.*, 584 (2005) 83.
39. J. A. Williams, C. B. Gorman, *Langmuir*, 23 (2007) 3103.
40. M. A. F. Addato, A. A. Rubert, G. A. Benítez, M. H. Fonticelli, J. Carrasco, P. Carro, R. C. Salvarezza, *J. Phys. Chem*. C, 115 (2011) 17788.
41. S. T. Marshall, D. K. Schwartz, J. W. Medlin, *Langmuir*, 27 (2011) 6731.
42. S. Bengió, M. Fonticelli, G. Benítez, A. H. Creus, P. Carro, H. Ascolani, G. Zampieri, B. Blum, R. C. Salvarezza, *J. Phys. Chem*. B, 109 (2005) 23450.
43. J. Oudar, P. Marcus, *Appl. Surf. Sci.*, 3 (1979) 48.
44. A. A. Wronkowska, *J. Electrochem. Soc.*, 140 (1993)1571.
45. A. A. Wronkowska, *Surf. Sci.*, 214 (1989) 507.
46. M. Iida, T. Ohtsuka, *Corros. Sci.*, 49 (2007) 1408.
47. Z. Mekhalif, J. Riga, J.-J. Pireaux, J. Dehalle, *Langmuir*, 13 (1997) 2285.
48. S. M. Kane, D. R. Huntley, J. L. Gland, *J. Phys. Chem*. B, 105 (2001) 9548.
49. L. Tortech, Z. Mekhalif, J. Delhalle, F. Guittard, S. Géribaldi, *Thin Solid Films*, 491 (2005) 253.

50. P. G. Hoertz, J. R. Niskala, P. Dai, H. T. Black, W. You, *J. Am. Chem. Soc.*, 130 (2008) 9763.
51. J. E. Sadler, D. S. Szumski, A. Kierzkowska, S. R. Catarelli, K. Stella, R. J. Nichols, M. H. Fonticelli, G. Benitez, B. Blum, R. C. Salvarezza, W. Schwarzacher, *Phys. Chem. Chem. Phys.*, 13 (2011) 17987.
52. B. Liu, F. Chen, L. Zheng, J. Ge, H. Xi and Y. Qian, *R.S.C. Adv.*, 3 (2013) 15075.
53. H. Grônbeck, A. Curioni, and W. Andreoni, *J. Am. Chem. Soc.*, 122 (2000) 3839.
54. A. P. Sandoval, J. M. Orts, A. Rodes, J. M. Feliu, *Electrochim. Acta*, 89 (2013) 72.
55. H. Grônbeck, *J. Phys. Chem.* C, 114 (2010) 15973.
56. D. K. Singh, E.-O. Ganbold, E.-M. Cho, C. M. Lee, S. I. Yang, S.-W. Joo, *J. Mol. Struct.*, 1049 (2013) 464.
57. P. Haider, A. Urakawa, E. Schmidt, A. Baiker, *J. Mol. Catal. A: Chem.*, 305 (2009) 161.
58. A. Johansson, S. Stafstrôm, *Chem. Phys. Lett.*, 322 (2000) 301.
59. G. R. Form and and E. S. Raper, T. C. Downie, *J. Acta Cryst.* B, 32 (1976) 345.
60. K. Ravikumar, K. C. Mohan, M. Bidyasagar, and G. Y. S. K. Swamy, *J. Chem. Cryst.*, 25 (1995) 325.
61. N. AlHokbany, I. Aljammaz, *O. J. I. C.*, 1 (2011) 23.
62. A. Kokalj, *Langmuir*, 26 (2010) 14582.
63. Y. Liu, M. Li, Y. Suo, *Surf. Sci.*, 600 (2006) 5117.
64. S. Yuan, C. Dai, J. Weng, Q. Mei, Q. Ling, L. Wang and W. Huang, *J. Phys. Chem.* A, 115 (2011) 4535.
65. D. Purdela, *J. Mol. Struct.*, 245 (1991) 119.
66. H. Schmidbaur, Gold: Progress in chemistry, biochemistry and technology, John Wiley, New York (1999).
67. A. Grohman and H. Schmidbaur, Comprehensive organometallic chemistry II, Vol. 3, In: E.W. Abel, F.G. Stone and G. Wilkinson eds, Elsevier Pergamon, Oxford (1995).
68. H. E. Abdou, A. A. Mohamed, and J. Fackler Jr., Gold(I) nitrogen chemistry, F. Mohr (Eds), gold chemistry: applications and future directions in the life sciences, Copyright c WILEY-VCH Verlag GmbH and Co. KGaA, Weinheim (2009) pp1–45.
69. M. C. Cimeno, A. Laguna, Comprehensive coordination chemistry II, Vol. 6, In Silver and Gold: J.A. McCleverty, T.J. Meyer, D.E. Fenton Eds, Elsevier Pergamon, Oxford UK (2004).
70. F. A. Cotton, Basic Inorganic Chemistry, Vol 3, John Willy and Sons, New York (1995).
71. M. Karelson, V. S. Lobanov, *Chem. Rev.,* 96 (1996) 1027.
72. G. Heimel, L. Romanerb, E. Zojerc, and J.-L. Brédasd, Organic optoelectronics and photonics III, *Proc. of SPIE*, 6999 (2008) 699919.
73. J. Sam and J. Abraham, *Ind. Eng. Chem. Res.*, 51 (2012) 16633.
74. G. Gece, *Corros. Sci.*, 50 (2008) 2981.
75. G. Bereket, C. Ogretir and A. Yurt, *J. Mol. Struct.* (THEOCHEM), 571 (2001) 139.
76. W. Cherry, N. Epiotis and W. Thatcher Borden, *Acc. Chem. Res.*, 10 (1977) 167.
77. M. Şahin, G. Gece, F. Karci, S. Bilgic, *J. Appl. Electrochem.*, 38 (2008) 809.
78. M. Lagrenée, B. Mernari, N. Chaibi, M. Traisnel, H. Vezin, F. Bentiss, *Corros. Sci.*, 43 (2001) 951.
79. K. F. Khaled, K. Babic´-samaradzija, N. Hackerman, *Appl. Surf. Sci.*, 240 (2005) 327.
80. O. Benali, L. Larabi, M. Traisnel, L. Gengembre, Y. Harek, *Appl. Surf. Sci.*, 253 (2007) 6130.
81. S. Baishya, R. C. Deka, *Comput.Theor. Chem.*, 1002 (2012) 1.
82. F. Zhang, Y. Tang, Z. Cao, W. Jing, Z. Wu and Y. Chen, *Corros. Sci.*, 61 (2012) 1.